ISSN 0023-1584, Kinetics and Catalysis, 2009, Vol. 50, No. 6, pp. 880–885. © Pleiades Publishing, Ltd., 2009.
Original Russian Text © O.B. Bel'skaya, V.A. Drozdov, T.I. Gulyaeva, A.B. Arbuzov, E.M. Moroz, D.A. Zyuzin, E.A. Paukshtis, T.V. Larina, V.K. Duplyakin, 2009, published in Kinetika i Kataliz, 2009, Vol. 50, No. 6, pp. 916–921.

Effect of Hydrothermal Treatment on the Composition and Structure of Pt(IV) Hydroxo Complexes As Model Precursors of the Active Component in Pt/Al_2O_3 Catalysts

O. B. Bel'skaya[a], V. A. Drozdov[a], T. I. Gulyaeva[a], A. B. Arbuzov[a], E. M. Moroz[b], D. A. Zyuzin[b], E. A. Paukshtis[b], T. V. Larina[b], and V. K. Duplyakin[b]

[a] *Institute of Hydrocarbon Processing, Siberian Branch, Russian Academy of Sciences, Omsk, 644040 Russia*
[b] *Boreskov Institute of Catalysis, Siberian Branch, Russian Academy of Sciences, Novosibirsk, 630090 Russia*
e-mail: obelska@rambler.ru

Received October 14, 2008

Abstract—The influence of hydrothermal treatment conditions (temperature, duration, acidity of the medium) on the structural and chemical transformations of the complex $H_2[Pt(OH)_6]$ was studied. The composition and structure of the resulting compounds were determined by several physicochemical methods. Thermal analysis coupled with mass spectrometry showed that, as the hydrothermal treatment temperature is raised from 25 to 120 and 150°C, the product composition in terms of empirical formulas changes as follows: $PtO_2 \cdot 4H_2O \longrightarrow PtO_2 \cdot 3.5H_2O \longrightarrow PtO_2 \cdot 1.5H_2O$. X-ray diffraction and UV and IR spectroscopy demonstrated that the changes in the chemical composition are accompanied by the amorphization of the structure and Pt–O bond strengthening. X-ray structure determination using the radial electron density distribution method showed that polynuclear species ~10–15 Å in size with a structure similar to that of orthorhombic PtO_2 form in the complexes subjected to "hard" hydrothermal treatment ($T \geq 150$°C).

DOI: 10.1134/S0023158409060147

Wide use of $Pt/\gamma\text{-}Al_2O_3$ catalysts in petroleum refining stimulates search for new methods and procedures for their preparation and integrated studies in this field. Priority is given to gaining insight into elementary steps and active site structure at the molecular level [1]. In recent years, non-chloride platinum compounds, for example, Pt(IV) hydroxo complexes, have been put forward as promising precursors of the active component in catalysts of this type [2]. Due to the strong binding of these complexes to the alumina surface via the coordination exchange of their OH ligands for hydroxyl groups of the oxide and due to their capability for forming polynuclear structures, a high degree of dispersion and preset geometry of active sites are attained already at the early stages of catalyst synthesis. Earlier, we proposed binding of platinum hydroxo complexes to $\gamma\text{-}Al_2O_3$ through the surface hydrolysis of a presorbed chloride precursor of platinum [3]. The approach is based on the hydrothermal treatment of the precursor at temperatures higher than 100°C. EXAFS and temperature-programmed reduction studies of the surface synthesis of the Pt(IV) hydroxo complexes [3] suggest that the hydrolysis of the starting chloroplatinate(IV) changes the character of the interaction between the anchored complex and the support and makes possible the formation of polynuclear platinum species on the surface via the formation of Pt–O(OH)–Pt bridges. For example, the EXAFS spectrum contains both the main peak indicating the existence of a Pt–O distance of 2.02 Å in the first coordination sphere and weaker peaks at 2.5–4.5 Å, whose intensity increases with increasing hydrothermal treatment temperature. These peaks are not due to stoichiometric platinum oxides and possibly indicate the formation of polynuclear complexes [3]. However, these structural data for the alumina-supported platinum complexes are rather difficult to interpret unambiguously.

The purpose of this work is to study the influence of hydrothermal treatment conditions on the composition and structure of the conversion products of model bulk samples of the platinum hydroxo complex $H_2[Pt(OH)_6]$ using a combination of physical methods.

EXPERIMENTAL

Synthesis and Hydrothermal Treatment of Model Samples

Hexahydroxoplatinic acid $H_2[Pt(OH)_6]$ was synthesized according to a known procedure [4] using $H_2[PtCl_6]$ as the starting compound. The product was identified by chemical and thermogravimetric analyses and X-ray diffraction. Bulk solid samples of the starting $H_2[Pt(OH)_6]$ complex, dried in air at room temperature, were placed in a titanium autoclave with

a glass insert, and water was added so that the solid-to-liquid ratio was 1 : 10. Hydrothermal treatment was carried out at 100, 120, or 150°C, and the treatment time was varied between 0.5 and 24 h. In particular cases, the medium was acidified to pH 3 by adding perchloric acid $HClO_4$, which did not change the composition of the coordination sphere of platinum in the starting complex.

Thermal analysis coupled with mass spectrometry (TA–MS). The TG–DTA method coupled with mass spectrometry was used to study the thermal decomposition of Pt(IV) hexahydroxo complex samples subjected to hydrothermal treatment under various conditions and to determine their composition. Intermediate compounds and thermal decomposition products were analyzed on an STA 449 C Jupiter thermal analyzer (Netzsch) connected to a QMS 403 C Aeolos quadrupole mass spectrometer with a heated capillary. Measurements were carried out in the dynamic mode in argon. The heating rate was 10 K/min. The sample weight was 10–20 mg.

Temperature-programmed reduction (TPR). Both the starting complex and hydrothermally treated samples were characterized by TPR. Before measurements with an AutoChem-2920 instrument (Micromeritics), the sample was purged with helium for 30 min at 25°C. Next, the helium flow was switched to a 10 vol % H_2 + Ar mixture (flow rate of 50 ml/min) and, after baseline stabilization, the sample was reduced while heating to 800°C at a rate of 10 K/min. The gases were 99.999 vol % pure.

Diffuse reflectance UV and IR spectroscopy. The diffuse reflectance spectroscopy (DRS) of powdered bulk complexes was carried out on a UV-2501 PC spectrophotometer (Shimadzu) with an ISR-240A diffuse reflectance attachment. The spectra were recorded in the 11000–54000 cm^{-1} range with $BaSO_4$ powder as the reference.

Diffuse reflectance IR (DRIFT) spectra were recorded on an FTIR-8300 Fourier spectrometer (Shimadzu) with a DRS-8000 attachment in the 400–6000 cm^{-1} range. The spectral resolution was 4 cm^{-1}, and the signal was accumulated from 50 scans. The spectra will be represented as the Kubelka–Munk function versus wave number.

X-ray diffraction. Diffraction patterns were recorded to determine the phase compositions of the starting complex $H_2[Pt(OH)_6]$ and the samples hydrothermally treated at 120, 150, and 190°C. The X-ray diffraction studies were carried out on a D8 Advance diffractometer (Bruker) in the $2\theta = 5°$ to 100° range using monochromated CuK_α radiation. The scan increment was 0.1°, and the counting time was 3 s per point. The diffraction patterns were interpreted using the ICDD database.

Radial electron density distribution (REDD). The X-ray structural study by the REDD method was carried out for identification of the structures of the compounds that resulted from the hydrothermal treatment of the starting $H_2[Pt(OH)_6]$ complex [5]. The X-ray diffraction pattern was obtained on a high-resolution diffractometer at the synchrotron irradiation station of the Institute of Nuclear Physics, Siberian Branch, Russian Academy of Sciences, using a Si(111) crystal monochromator placed in the diffraction beam, which selected the wavelength $\lambda = 1.1$ Å and provided a degree of monochromation of $\Delta\lambda/\lambda \sim 10^{-4}$. Scans were made in a Bragg angle range of $2\theta = 5°$–135°. REDD curves were calculated as described in [5] and were then compared with the model curves of crystalline $H_2[Pt(OH)_6]$ and known platinum oxides of different compositions and structures. Structural data from the ICSD/Retrieve database were used. Interatomic distances and coordination numbers were calculated using the same program.

RESULTS AND DISCUSSION

Thermal Decomposition and Temperature-Programmed Reduction of $H_2Pt(OH)_6$ before and after Hydrothermal Treatment under Various Conditions

An analysis of the TG–DTG–DTA–MS curves shows that two main decomposition regions, with endotherms at 100–300 and 450–600°C corresponding to the release of water and oxygen, respectively, are observed for all samples (Fig. 1). Since the platinum metal phase, detected by X-ray diffraction, is formed at the end of thermal analysis, the weight losses observed in the high-temperature region, accompanied by oxygen evolution, are due to the decomposition of the oxide formed at the first stage: $PtO_2 \longrightarrow Pt + O_2$. Representing the starting complex and the compounds formed from this complex under different hydrothermal conditions as $PtO_2 \cdot nH_2O$, we determined empirical formulas for each of the samples examined:

1. Starting complex $H_2[Pt(OH)_6] - PtO_2 \cdot 4H_2O$;

2. Complex after hydrothermal treatment at 120°C for 3 h–$PtO_2 \cdot 3.5H_2O$;

3. Complex after hydrothermal treatment in an acidic medium at 120°C for 3 h–$PtO_2 \cdot 2.2H_2O$;

4. Complex after hydrothermal treatment at 150°C for 3 h–$PtO_2 \cdot 1.5H_2O$.

It was thus found that an increase in the hydrothermal treatment temperature substantially changes the composition of the starting Pt(IV) hydroxo complex and, first of all reducing the amount of structural water as H^+ and OH^- groups. The hydrothermal treatment of the complex in an acidic medium at the same temperature results in a deeper dehydration of the complex. It can be assumed that this increases the proportion of the PtO_2-type "oxide-like" structure resulting from the hydrothermal treatment.

The TPR profiles of the starting $H_2[Pt(OH)_6]$ complex and the samples subjected to hydrothermal treatment at 120 and 150°C for 3 h are shown in Fig. 2. The

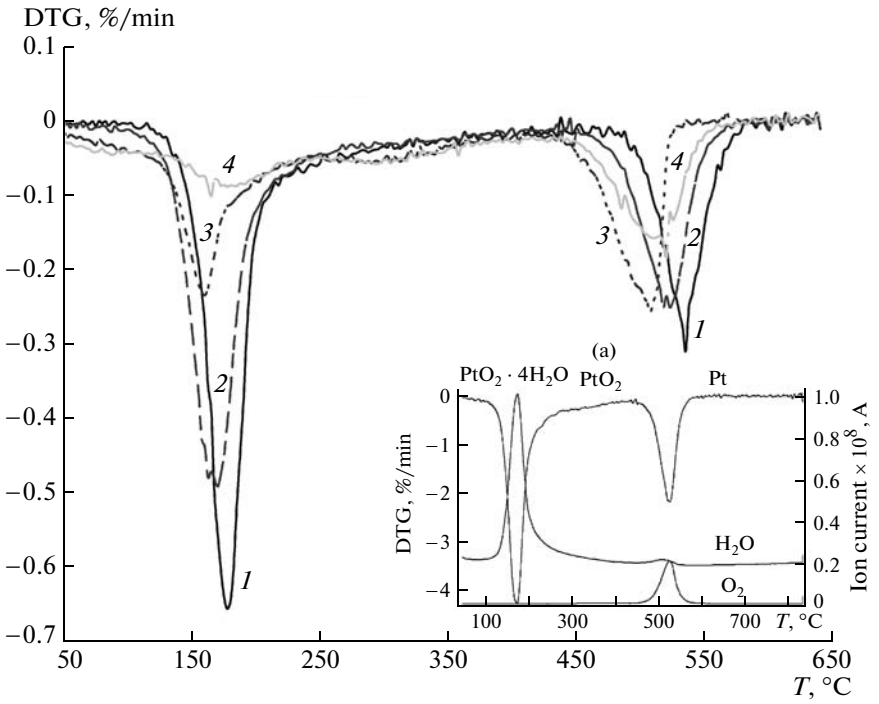

Fig. 1. DTG curves of (*1*) the starting hydroxo complex $H_2[Pt(OH)_6]$ and (*2*–*4*) the samples subjected to hydrothermal treatment at (*2*, *3*) 120°C (*3*, acidic medium) and (*4*) 150°C. (a) Typical mass spectrum of the decomposition products: H_2O, $m/e = 18$; O_2, $m/e = 32$.

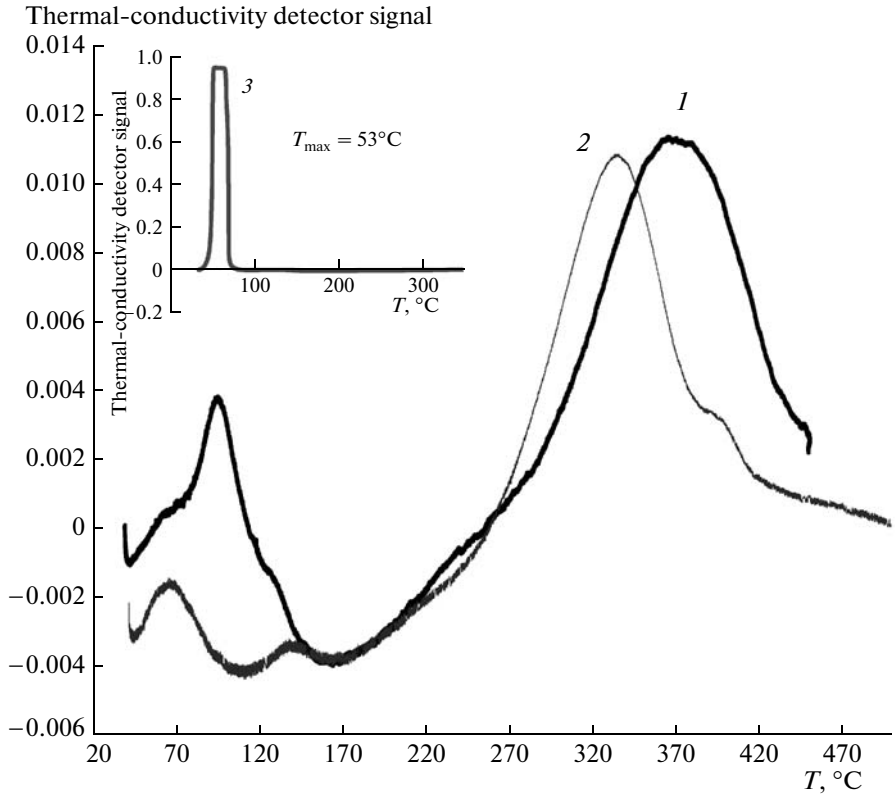

Fig. 2. TPR curves of (*1*) the complex after hydrothermal treatment at 120°C for 3 h, (*2*) the complex after the hydrothermal treatment at 150°C for 6 h, and (*3*) (inset) the starting complex $H_2[Pt(OH)_6]$.

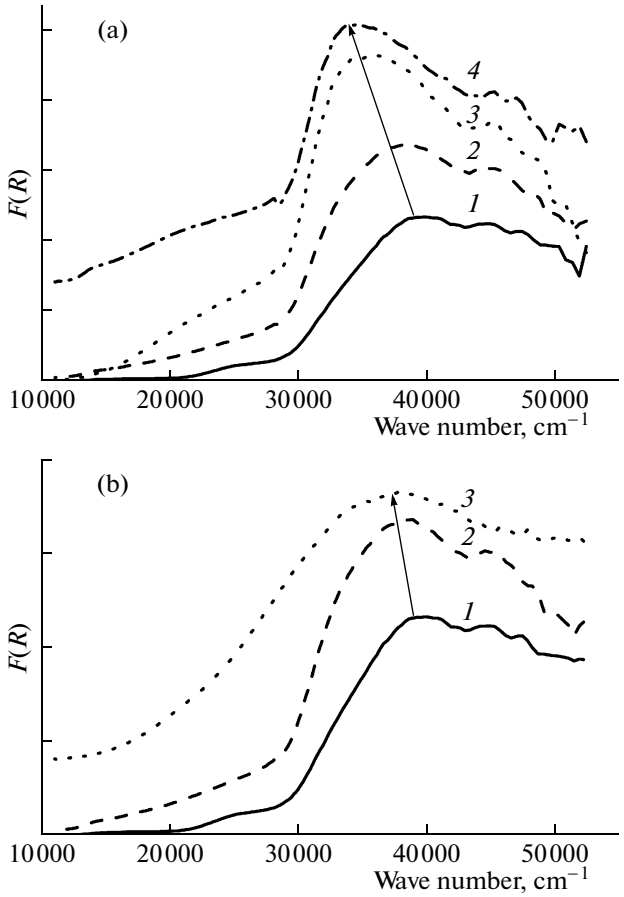

Fig. 3. (a) Changes in the DRS spectra of the samples with hydrothermal treatment temperature: (*1*) the starting complex $H_2[Pt(OH)_6]$, (*2*) the complex after hydrothermal treatment at 120°C for 3 h, (*3*) the complex after hydrothermal treatment at 120°C for 3 h in an acidic medium, and (*4*) the complex after hydrothermal treatment at 150°C for 6 h. (b) Changes in the DRS spectra of the samples with the hydrothermal treatment time: (*1*) the starting complex $H_2[Pt(OH)_6]$, (*2*) the complex after hydrothermal treatment at 120°C for 3 h, and (*3*) the complex after hydrothermal treatment at 120°C for 24 h.

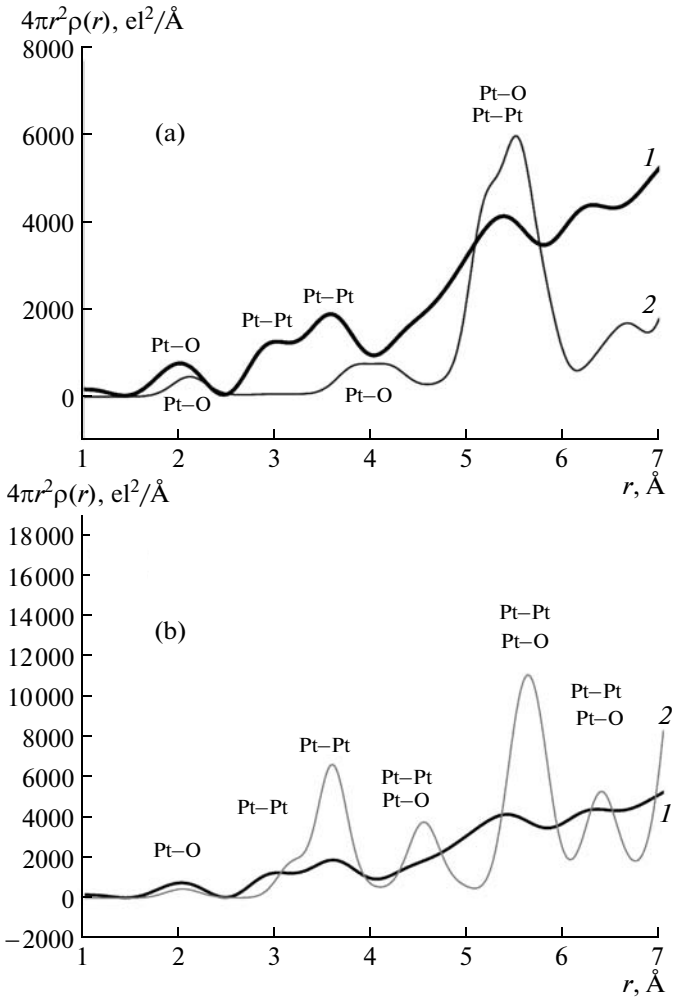

Fig. 4. Radial electron density distribution curves of the samples: (a) (*1*) experimental REDD curve for $H_2[Pt(OH)_6]$ after hydrothermal treatment at 150°C and (*2*) calculated REDD curve of the starting $H_2[Pt(OH)_6]$ complex; (b) (*1*) experimental REDD curve of the complex after hydrothermal treatment at 150°C and (*2*) REDD curve calculated for PtO_2.

$H_2[Pt(OH)_6]$ complex is readily reducible with hydrogen already between 40 and 70°C (T_{max} = 53°C), whereas the character of reduction of the samples after hydrothermal treatment is substantially different. The complicated character of the TPR curves of the samples subjected to hydrothermal treatment is likely due to their heterogeneous composition and structure. For example, along with the readily reducible residues of fragments of the starting complex structure, larger, polynuclear, mixed oxo and hydroxo structures are formed, and they are difficult to reduce under the TPR conditions for both thermodynamic and kinetic reasons.

Diffuse Reflectance UV and IR Spectroscopy Data

The diffuse reflectance UV and IR spectra of the complexes are shown in Fig. 3. The absorption bands at 25000 and 38000 cm^{-1} appear in the spectrum of the starting $H_2[Pt(OH)_6]$, indicating the presence of octahedrally coordinated Pt^{4+} [6]. Hydrothermal treatment results in a shift of the absorption band at 38000 cm^{-1} to lower wave numbers (34000 cm^{-1}) and in an increase in the absorption intensity below 28000 cm^{-1}. These effects strengthen monotonically with an increase in the treatment temperature from 120 to 150°C (Fig. 3a) and in the treatment time from 3 to 24 h at a given temperature (Fig. 3b). The data in Fig. 3 show that the changes induced by thermal treatment at 150°C can be produced by treatment under milder conditions (120°C) but in an acidic medium. Thus, it was found by DRS that all of the three factors (temperature, time, and acidity of the medium) cause similar changes in the spectral characteristics, specifically, a shift of absorption bands to lower wave num-

bers and an increase in the absorption intensity in the low-frequency region. These changes are consistent with the assumption that hydrothermal treatment causes enlargement of the complex particles [7] and the formation of "oxide-like" structures [8], including by oxygen bridging of platinum atoms.

According to DRIFT data, the starting $H_2[Pt(OH)_6]$ sample is characterized by a broad absorption band at 3200–3300 cm^{-1} due to OH groups, an absorption band at 1015 cm^{-1} due to the bending vibrations of the Pt–OH bond, and a weak absorption band at 447 cm^{-1} assigned to the Pt–O bond. The broadness of the absorption band at 3200–3300 cm^{-1} indicates a strong perturbation of the OH groups by hydrogen bonding. The transformation of this complex caused by the variation of temperature, time, and the acidity of the medium in hydrothermal treatment is characterized primarily by Pt–O bond strengthening up to the formation of a double (or bridging) Pt=O (Pt–O–Pt) bond with a decrease in the number of the Pt–OH groups [9], by the disappearance of the hydrogen-bonded OH groups, and by the formation of water molecules. For example, hydrothermal treatment at 120°C (both with and without acidification of the aqueous phase to pH 3) and at 150°C shifts the Pt–O band of from 447 to 636 and 705 cm^{-1}, respectively. In the region of absorption of the hydrogen-bonded OH groups, a narrower band at 3477 cm^{-1} appears instead of the broad band at 3200–3300 cm^{-1}. This can be due to the weakening of the bonds between particular $[Pt(OH)_6]^{2-}$ anions. The spectra of the samples subjected to hydrothermal treatment, particularly those of the samples treated in the acidic medium, exhibit additional absorption bands of molecular water (1630 and 3470 cm^{-1}). Thus, the IR spectroscopic data do not contradict the assumption about the rearrangement of the $[Pt(OH)_6]^{2-}$ anions under the hydrothermal conditions with the formation of structures with a bridging oxygen atom, Pt–O–Pt.

X-Ray Diffraction Data

According to X-ray diffraction data, the starting $H_2[Pt(OH)_6]$ complex has a monoclinic crystal structure. The structure is amorphized as the hydrothermal treatment temperature increases, and this process is more pronounced in the acidic medium. The crystallinity of $H_2[Pt(OH)_6]$ remains unchanged upon hydrothermal treatment at 120°C, while at 150°C the product is dominated by a phase amorphous to X-rays. To determine its structure, the experimental REDD curves of the sample was obtained and compared with the calculated model REDD curve of $H_2[Pt(OH)_6]$ (ICSD/Retrieve, no. 8256). An analysis of the curves (Fig. 4a) shows that the structure of the sample (hydrothermal treatment at 150°C) cannot be described in terms of the $H_2[Pt(OH)_6]$ structure, because the model curve contains no coordination peaks at 2.9–3.7 Å present in the experimental curve. It can be assumed that these peaks are due to Pt–Pt distances. A comparison of the experimental curve with the model curves of platinum oxides of different compositions and structures (Fig. 4b) revealed that the maximum similarity of peak positions is observed for the REDD curve of the sample and the REDD curve of orthorhombic PtO_2 (ICSD/Retrieve, no. 24925). The decrease in the coordination numbers for the Pt–Pt distances in the 2.9–3.7 Å range indicates strong structural disordering and a small particle size. Based on the decrease in the coordination number, the characteristic half-width of the halo in the X-ray diffraction pattern, and the characteristic distance in the REDD curve at which coordination peaks can be distinguished reliably, we can state that the particle size is ~10–15 Å, which is equal to the size of 2–3 unit cells of orthorhombic platinum(IV) oxide.

The above data suggest the following structural model for the $H_2[Pt(OH)_6]$ complex subjected to hydrothermal treatment, allowing the formation of Pt–O(OH)–Pt bonds:

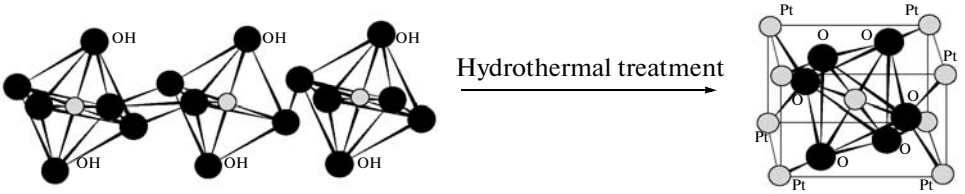

Fragment of the $H_2[Pt(OH)_6]$ structure

Structure of $H_2[Pt(OH)_6]$ after hydrothermal treatment

ACKNOWLEDGMENTS

This work was supported by the Russian Foundation for Basic Research, project no. 06-03-32862.

REFERENCES

1. Bel'skaya, O.B. and Duplyakin, V.K., *Ross. Khim. Zh.*, 2007, vol. 51, no. 4, p. 29.

2. Lisitsin, A.S., Okhlopkova, O.B., Bel'skaya, O.B., and Duplyakin, V.K., *Tezisy dokl. konf. "Molekulyarnyi dizain katalizatorov i kataliz v protsessakh pererabotki uglevodorodov i polimerizatsii* (Proc. Conf. on Molecular Design of Catalysts and Catalysis in Hydrocarbon Processing and Polymerization), Omsk, 2005, p. 42.
3. Bel'skaya, O.V., Karymova, R.Kh., Kochubei, D.I., and Duplyakin, V.K., *Kinet. Katal.*, 2008, vol. 49, no. 5, p. 764 [*Kinet. Catal.* (Engl. Transl.), vol. 49, no. 5, p. 720].
4. *Sintez kompleksnykh soedinenii metallov platinovoi gruppy: Spravochnik* (Synthesis of Platinum Metal Complexes: A Handbook), Moscow: Nauka, 1964.
5. Moroz, E.M., *Russ. Chem. Rev.*, 1992, vol. 61, p. 188.
6. Buslaeva, T.M., Umreiko, D.S., Novitskii, G.G., et al., *Khimiya i spektroskopiya galogenidov platinovykh metallov* (Chemistry and Spectroscopy of Platinum Metal Halides), Minsk: Universitetskoe, 1990, p. 68.
7. Ershov, B.G. and Sukhov, N.L., *Zh. Fiz. Khim.*, 2001, vol. 75, no. 8, p. 1430 [*Russ. J. Phys. Chem.* (Engl. Transl.), vol. 75, no. 8, p. 1303].
8. Lieske, H., Lietz, G., Spindler, H., and Volter, Y., *J. Catal.*, 1983, vol. 81, no. 1, p. 8.
9. Maya, L., Riester, L., Thundat, T., and Yust, C.S., *J. Appl. Phys.*, 1998, vol. 84, no. 11, p. 6382.